Choriocapillaris in Age-Related Macular Degeneration: A Systematic Review of Optical Coherence Tomography Angiography–Based Assessments and Challenges in

Choriocapillaris in Age-Related Macular Degeneration: A Systematic Review of Optical Coherence Tomography Angiography–Based Assessments and Challenges in Standardization

ALESSANDRO BERNI, CLAUDIO FOTI, LORENA ULLA, CHINMAYI VYAS, JAY CHHABLANI, VARUN CHAUDHARY, YOUSIF SUBHI, GIOVANNI GREGORI, RUIKANG K. WANG, PHILIP J. ROSENFELD, SRINIVAS R. SADDA, FRANCESCO BANDELLO, MICHELE REIBALDI, AND ENRICO BORRELLI

• TOPIC: This systematic review evaluates the methodologies used for assessing the choriocapillaris (CC) in age-related macular degeneration (AMD) using optical coherence tomography angiography (OCTA). It focuses on identifying methodological heterogeneity in imaging and analysis protocols and its implications for clinical and research applications.

• CLINICAL RELEVANCE: AMD is a leading cause of vision loss, and assessing CC perfusion provides critical insights into its pathophysiology. OCTA has emerged as a noninvasive imaging technique offering high-resolution visualization of the CC. However, variability in methodologies has hindered the standardization of CC assessments. Establishing consistent practices is essential for improving clinical and research outcomes in AMD management.

• DESIGN: Systematic review.

• METHODS: Studies included in this review were selected on the basis of eligibility criteria defined by the Population, Intervention, Comparator, Outcome, Study design framework. Participants included patients with early, intermediate, and late AMD. Interventions involved the use of OCTA for CC assessment, with no restrictions on device type or scan parameters. Comprehensive searches of MEDLINE, Web of Science Core Collection, and the Cochrane Library were conducted up to November 30, 2024. Data extractions and narrative synthesis focused on device types, scan protocols, segmentation techniques, compensation strategies, and quantitative metrics.

• RESULTS: A total of 102 studies, encompassing 4047 patients with AMD and 4415 eyes, were analyzed. Fifty-two studies used spectral-domain OCTA, and 49 studies used swept-source OCTA, with significant heterogeneity in segmentation boundaries and slab thickness (4.4-30 μm). Only 32 studies used compensation strategies to address signal attenuation under drusen. Quantitative metrics varied widely, with CC flow deficit percentage being the most common. However, inconsistencies in thresholding methods and lack of standardized Phansalkar radius reporting limited comparability. The review highlights gaps in reporting segmentation boundaries and compensation techniques, which impact the ability to assess the reliability of findings.

• CONCLUSIONS: This review underscores substantial variability in methodologies for CC assessment in AMD, highlighting the urgent need for standardized imaging protocols and analytical approaches. Despite advances in OCTA technology, inconsistencies in segmentation, thresholding, and compensation strategies challenge data reliability and reproducibility. Future research should prioritize methodological standardization to enhance comparability and clinical applicability. (Am J Ophthalmol 2025;277: 482–496.

AJO.com Supplemental Material available at AJO.com.
Accepted for publication May 29, 2025.

From the IRCCS San Raffaele Scientific Institute, Milan, Italy (A.B., F.B.); Vita-Salute San Raffaele University, Milan, Italy (A.B., F.B.); Department of Surgical Sciences, University of Turin, Turin, Italy (C.F., L.U., M.R., E.B.); Department of Ophthalmology, "City of Health and Science" Hospital, Turin, Italy (C.F., L.U., M.R., E.B.); Division of Ophthalmology, Department of Surgery, McMaster University, Hamilton, Ontario, Canada (C.V., V.C.); Department of Ophthalmology, University of Pittsburgh School of Medicine, Pittsburgh, Pennsylvania, USA (J.C.); Department of Health Research Methods, Evidence and Impact, McMaster University, Hamilton, Ontario, Canada (V.C.); Department of Ophthalmology, Rigshospitalet, Copenhagen, Denmark (Y.S.); Department of Clinical Research, University of Southern Denmark, Odense, Denmark (Y.S.); Department of Clinical Medicine, University of Copenhagen, Copenhagen, Denmark (Y.S.); Department of Ophthalmology, Bascom Palmer Eye Institute, University of Miami Miller School of Medicine, Miami, Florida, USA (G.G., P.J.R.); Department of Bioengineering, University of Washington, Seattle, Washington, USA (R.K.W.); Department of Ophthalmology, University of Washington, Seattle, Washington, USA (R.K.W.); Department of Ophthalmology, David Geffen School of Medicine at UCLA, Los Angeles, California, USA (S.R.S.); Doheny Eye Institute, Pasadena, California, USA (S.R.S.); Department of Ophthalmology, Faculty of Medicine, Biruni University, İstanbul, Turkey (E.B.)

Inquiries to Enrico Borrelli, Department of Ophthalmology, University of Turin, Turin, Italy; e-mail: borrelli.enrico@yahoo.com

0002-9394/$36.00
https://doi.org/10.1016/j.ajo.2025.05.051

INTRODUCTION

Age-related macular degeneration (AMD) is a leading cause of vision loss in the elderly.[1-3] AMD may be classified into different stages: early AMD (ie, drusen >63 μm), intermediate AMD with large drusen (>125 μm) or pigmentary abnormalities, and late AMD characterized by the presence of macular neovascularization or geographic atrophy (GA).[1,4]

Although the precise mechanisms underlying AMD remain unclear, research indicates that its development and progression are influenced by a combination of factors, including oxidative stress, environmental influences, and genetic predisposition.[5,6] Despite the complexity of these mechanisms, AMD ultimately leads to alterations in the unit formed by the photoreceptors, retinal pigment epithelium (RPE), Bruch's membrane (BM), and the choriocapillaris (CC). Changes in the CC have been identified as a significant biomarker of AMD, as evidenced by histopathological studies.[7-10] Advances in imaging technologies have significantly improved our ability to study the CC, particularly through optical coherence tomography angiography (OCTA).[7] Specifically, the latter imaging modality may offer high-resolution visualization of the CC, enabling qualitative and quantitative assessment of its perfusion.[11] As a result, numerous studies using OCTA to investigate CC changes in patients with AMD have been published.

Although OCTA has significantly enhanced our ability to evaluate the CC, this assessment is not without challenges. Lesions commonly associated with AMD, such as drusen and areas of hypopigmentation or hyperpigmentation, can generate shadow artifacts. In this context, swept-source (SS) OCTA systems, with their longer wavelengths, offer improved penetration through the RPE, reducing the effect of shadowing artifacts and enhancing the visualization of the CC in AMD eyes compared with spectral-domain (SD) OCTA systems, primarily due to reduced optical scattering in retinal tissue at longer wavelengths. Additionally, quantifying CC perfusion involves algorithms that vary in their approaches, including differences in the slabs used for CC visualization, binarization thresholds, brightness/contrast adjustments, and methods for compensating signal attenuation using structural information. Some algorithms also account for the tailing effect caused by overlying highly scattering materials, such as calcified drusen, which can generate ghost signals at the CC.[12] Although existing reviews primarily describe CC changes in AMD, no systematic reviews have been published to examine the methodologies used for CC assessment in these patients. To address this gap, our research systematically investigated the various methodologies used for CC assessment in AMD. By examining these approaches, we aim to uncover the heterogeneity in CC assessments for AMD and emphasize the need for standardization in CC assessment methodologies.

METHODS

• **REVIEW PROTOCOL AND REGISTRATION:** This systematic review adhered to the Preferred Reporting Items for Systematic Reviews and Meta-Analyses guidelines. The protocol for the review was registered with the International Prospective Register of Systematic Reviews (PROSPERO, CRD42024627204).

• **ELIGIBILITY CRITERIA AND OUTCOMES:** Study eligibility was defined using the Population, Intervention, Comparator, Outcome, Study design framework.

Population (P): Patients diagnosed with any stage of AMD, including early AMD, intermediate AMD, neovascular AMD, and GA. There were no restrictions on age, gender, or ethnicity.

Intervention (I): Studies using OCTA to evaluate CC. Studies using any type of OCTA device, including SD- and SS-OCTA, with any scan sizes, were eligible.

Comparator (C): Methodological comparisons (eg, differences in devices, scan sizes, segmentation approaches) were also eligible. Studies without explicit comparators were included if they satisfied other criteria.

Outcome (O): Outcomes focused on methodological details and metrics for assessing CC perfusion or nonperfusion. Key parameters included segmentation boundaries, segmentation techniques, manual corrections, thresholding methods, and image analysis metrics such as flow deficit (FD) density, perfusion density, and vessel density (VD).

Study Design (S): Prospective or retrospective studies focused on AMD and OCTA-based CC assessments were eligible. Review articles, commentaries, editorials, meeting abstracts, case reports, and studies lacking sufficient methodological or result details were excluded.

• **SEARCH STRATEGY:** On November 1, 2024, the authors conducted a systematic search to capture references on PubMed, Web of Science Core Collection, and the Cochrane Library published from inception. The search was updated on November 30, 2024, to identify any new publications. The search involved MeSH headings and text-term mapping to AMD and CC and equivalents as shown in Supplementary Table 1.

The initial electronic search was augmented by a further manual search of the reference lists from included studies. Citations were captured and exported to Covidence for further screening. Two reviewers independently performed the search (C.F. and L.U.). Disagreements were resolved through discussion with a senior reviewer (E.B.) who

would provide a final decision if consensus could not be reached.

• **STUDY SELECTION AND DATA COLLECTION:** Two reviewers (C.F. and L.U.) screened titles and abstracts independently based on predefined inclusion and exclusion criteria. Full-text reviews were conducted for eligible studies, with disagreements resolved through discussion with a senior reviewer (E.B.) who would provide a final decision if consensus could not be reached. The study selection process is summarized in a Preferred Reporting Items for Systematic Reviews and Meta-Analyses flow diagram.

Data extraction was carried out independently by 2 reviewers (C.F. and L.U.) using a predefined, pilot-tested data collection form. All extracted data were recorded in Microsoft Excel (Version 16.93.1). The extracted information included study details, patient characteristics, OCTA scan parameters, choriocapillaris segmentation strategy and boundaries, image processing techniques and analytical methods, and outcome measures.

Discrepancies were resolved by discussion or consultation with a senior reviewer (E.B.) who would provide a final decision if consensus could not be reached.

• **STRATEGY FOR DATA SYNTHESIS:** A qualitative synthesis was conducted to describe the methodology used within the studies, including differences in imaging devices, protocols, and analysis techniques. The synthesis focused on summarizing methodologies while identifying trends and inconsistencies. The heterogeneity of outcomes did not allow for a meaningful meta-analysis.

RESULTS

The literature search retrieved 3971 studies after removing duplicates. After title and abstract screening, 369 articles remained. Of these, 102 studies met the inclusion criteria and were included in the review (Figure 1).[2,8,12-111] The selected studies were published between 2014 and 2024. The included studies analyzed data from 4415 unique eyes across 4047 patients with AMD, comprising 2693 eyes with early or intermediate dry AMD, 913 eyes with neovascular AMD, and 809 eyes with late dry AMD.

• **OCTA DEVICES:** A total of 52 studies used SD devices to analyze the CC, and 49 studies used SS devices. Only 1 study directly compared SS-OCTA and SD-OCTA, using a 400 kHz prototype SS device and the RTVue XR Avanti (Optovue). Among the studies using SS-OCTA, the most frequently used device was the PLEX Elite 9000 (Carl Zeiss Meditec) in 38 studies, followed by the DRI OCT Triton (Topcon Corporation) in 9 studies, and a 400 kHz ultra-high-speed prototype device in 3 studies. For SD-OCTA, the RTVue XR Avanti (Optovue) was the most commonly used device in 34 studies, followed by the Cirrus 5000 (Carl Zeiss Meditec) in 12 studies, the Spectralis HRA+OCT (Heidelberg Engineering) and the Solix (Optovue) in 3 studies each, and the Nidek Mirante (Nidek) in 1 study.

• **SCAN PROTOCOLS:** The most commonly used OCTA scan size for evaluation of CC was 6×6 mm, used in 57 studies, followed by 3×3 mm in 46 studies. Other scan sizes were used far less frequently: 4.5×4.5 mm in 4 studies, 6.4×6.4 mm in 3 studies, 2×2 mm in 3 studies, 4.4×4.4 mm in 2 studies, and 6×4.5 mm and 8×8 mm in 1 study each. All scans were centered on the fovea.

• **SEGMENTATION:** The segmentation boundaries used to assess the CC varied widely across the included studies, with notable differences in the inner and outer boundaries, as well as slab thickness (Table 1).

BM was the reference layer for both the superior and inferior boundaries in 42 studies, with CC slab thicknesses ranging from 4.4 μm to 30 μm. In 14 studies, the inner boundary was placed directly at the BM. Among these, the outer boundary was positioned at 20 μm below BM in 8 studies, 10.4 μm below in 4 studies, 25 μm below in 1 study, and 30 μm below in 1 study. In 11 studies, the inner boundary was placed 4 μm beneath BM, with the outer boundary positioned at 20 μm below BM in 8 studies, 16 μm below in 1 study, 19 μm below in 1 study, and 24 μm below in 1 study. In 6 studies, the inner boundary was placed 10 μm beneath BM, with the outer boundary positioned at 30 μm below BM in 4 studies and 18 μm below in 2 studies. Other reported ranges included 10.4 to 20.8 μm (1 study), 3 to 30 μm (1 study), 5 to 25 μm (1 study), 9 to 30 μm (1 study), 9 to 31 μm (1 study), 21 to 31 μm (1 study), 26 to 49 μm (1 study), and 30 to 60 μm (1 study). Additionally, 2 studies did not specify the exact positioning of the boundaries but reported a slab thickness of 4.4 μm with reference to BM.

The RPE layer (without specifying whether the inner or outer boundary was considered) was used as the reference layer in 13 studies, with CC slab thicknesses ranging from 8 μm to 30 μm. In 7 studies, the inner boundary was placed 31 μm below the RPE. Among these, the outer boundary was positioned at 61 μm below the RPE in 3 studies, 41 μm below in 3 studies, and 59 μm below in 1 study. In 2 studies, the inner boundary was placed directly at the RPE, with the outer boundary positioned 10 μm below in 1 study and 20 μm below in another. Two studies defined the slab as spanning 29 to 49 μm beneath the RPE, and 1 study used 29 to 37 μm. One study positioned the inner boundary 30 μm below the RPE and the outer boundary 60 μm below the RPE.

Two studies used the RPE centerline as the reference layer, placing the inner boundary at 31 μm below it and

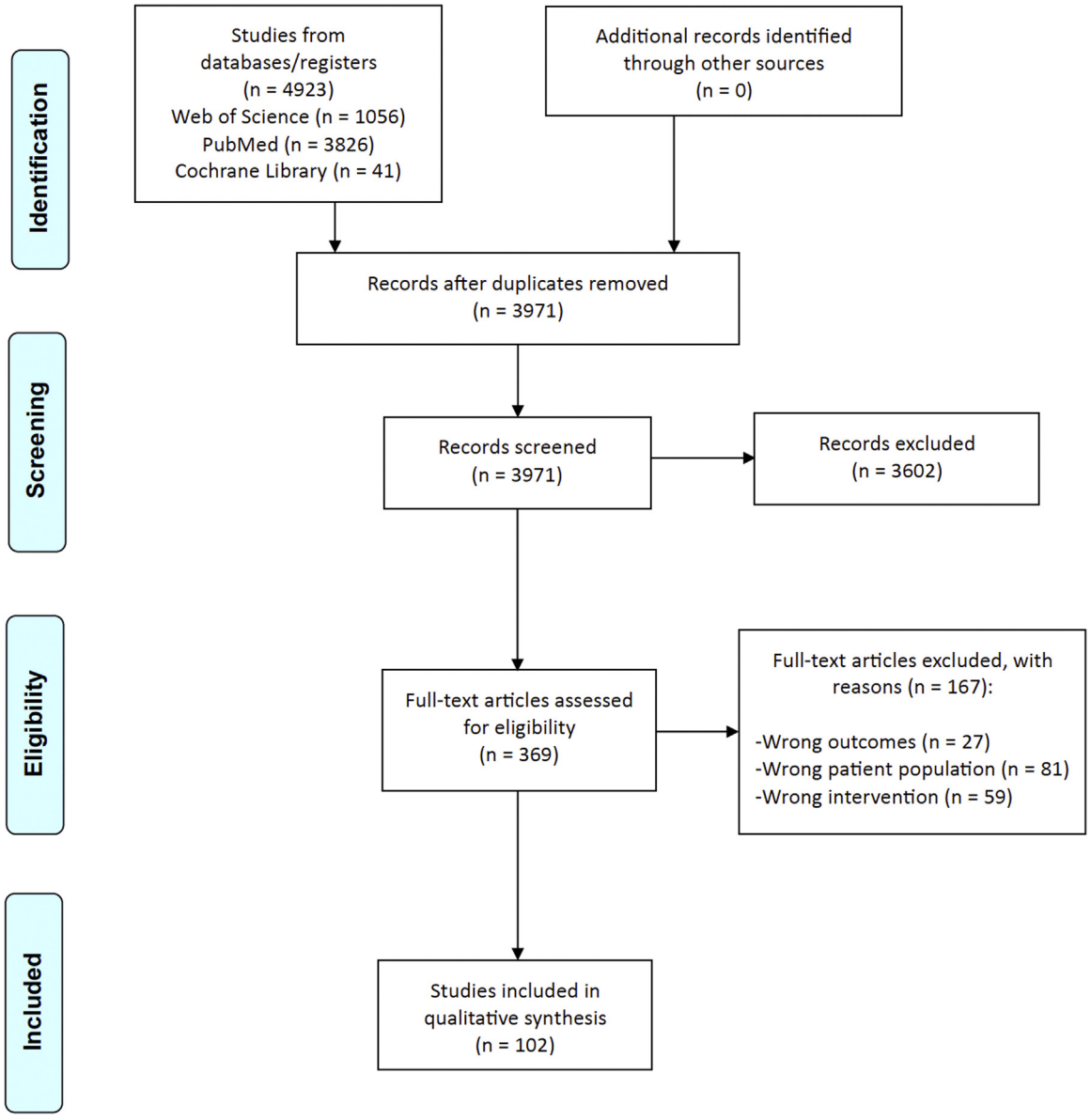

FIGURE 1. Preferred Reporting Items for Systematic Reviews and Meta-Analyses flow diagram of study selection process.

the outer boundary at 41 µm below in 1 study and 61 µm in 1 study.

One study instead used the inner limit of the RPE line as the reference, with boundaries placed 30 and 40 µm below, respectively.

The RPE fit, which approximates the inner boundary of BM, was used as the reference layer in 12 studies. In 5 of these studies, the inner boundary was placed 31 µm beneath the RPE fit, with the outer boundary positioned at 41 µm below BM. Two studies placed the inner boundary 10 µm below the RPE fit, with the outer boundary positioned at 31 µm in 1 study and 40 µm in another. Another study reported a range of 21 to 31 µm beneath the RPE fit. One study used the RPE fit as the inner boundary and BM as the outer boundary, and another study defined the slab as spanning 16 to 31 µm beneath the RPE fit. Figure 2 shows how the choice of different segmentation boundaries affects the appearance of the en face CC slabs and influences CC metrics quantification.

Additionally, 2 studies used the RPE-BM complex as the reference layer. In 1 study, the boundaries spanned 16 to 31 µm beneath the complex, whereas in the other study, the slab extended from 31 to 41 µm below it.

Five studies reported only the slab thickness without specifying a reference layer, with thicknesses of 10 µm in 2 studies, 20 µm in 2 studies, and 40 µm in 1 study.

Finally, the accuracy of the segmentation boundaries was not reported in 26 studies.

Only 61 studies reported manually adjusting the segmentation when the automated segmentation, either built-

TABLE 1. Segmentation Boundaries Used for the Definition of Choriocapillaris Slabs in the Included Studies

Inner Boundary Position	Outer Boundary Position	No. of Studies
BM	10.4 μm below BM	4
BM	20 μm below BM	8
BM	25 μm below BM	1
BM	30 μm below	1
3 μm below BM	30 μm below BM	1
4 μm below BM	16 μm below	1
4 μm below BM	19 μm below	1
4 μm below BM	20 μm below	8
4 μm below BM	24 μm below	1
5 μm below BM	25 μm below BM	1
9 μm below BM	30 μm below	1
9 μm below BM	31 μm below BM	1
10 μm below BM	18 μm below	2
10 μm below BM	30 μm below	4
10.4 μm below BM	20.8 μm below BM	1
21 μm below BM	31 μm below BM	1
26 μm below BM	49 μm below BM	1
30 μm below BM	60 μm below BM	1
30 μm below RPE inner limit	40 μm below RPE inner limit	1
RPE	10 μm below RPE	1
RPE	20 μm below RPE	1
31 μm below RPE	41 μm below RPE	3
31 μm below RPE	61 μm below RPE	3
31 μm below RPE	59 μm below RPE	1
29 μm below RPE	37 μm below RPE	1
29 μm below RPE	49 μm below RPE	2
30 μm below RPE	60 μm below RPE	1
31 μm below RPE centerline	41 μm below RPE centerline	1
31 μm below RPE centerline	61 μm below RPE centerline	1
RPE fit	BM	1
10 μm below RPE fit	31 μm below RPE fit	1
10 μm below RPE fit	40 μm below RPE fit	1
16 μm below RPE fit	31 μm below RPE fit	1
21 μm below RPE fit	31 μm below RPE fit	1
31 μm below RPE fit	41 μm below RPE fit	5
16 μm below RPE-BM complex	31 μm below RPE-BM complex	1
31 μm below RPE-BM complex	41 μm below RPE-BM complex	1
Slab Thickness With No Reported Boundaries		
4.4 μm (with reference to BM)		1
10 μm (no reference)		2
20 μm (no reference)		2
40 μm (no reference)		1

BM = Bruch's membrane; RPE = retinal pigment epithelium.

in or provided by external software, was deemed inaccurate.

• **COMPENSATION:** Thirty-two of 102 studies reported using a compensation strategy to account for signal attenuation under drusen. All studies followed the methodology proposed by Zhang and associates in 2018,[40] which consists of using the inverted structural signal from the CC structural slab to restore the signal in areas under drusen where it has been attenuated. In detail, the CC structural slab is first inverted and then multiplied by the CC flow slab to obtain the compensated CC flow image where the attenuation artifacts due to drusen are mitigated. This process has been validated in drusen-resolving eyes, providing the same CC status both before and after drusen reabsorption, but has not been validated or proved effective in restoring the signal under other structures like hyperreflective foci or calcified drusen.

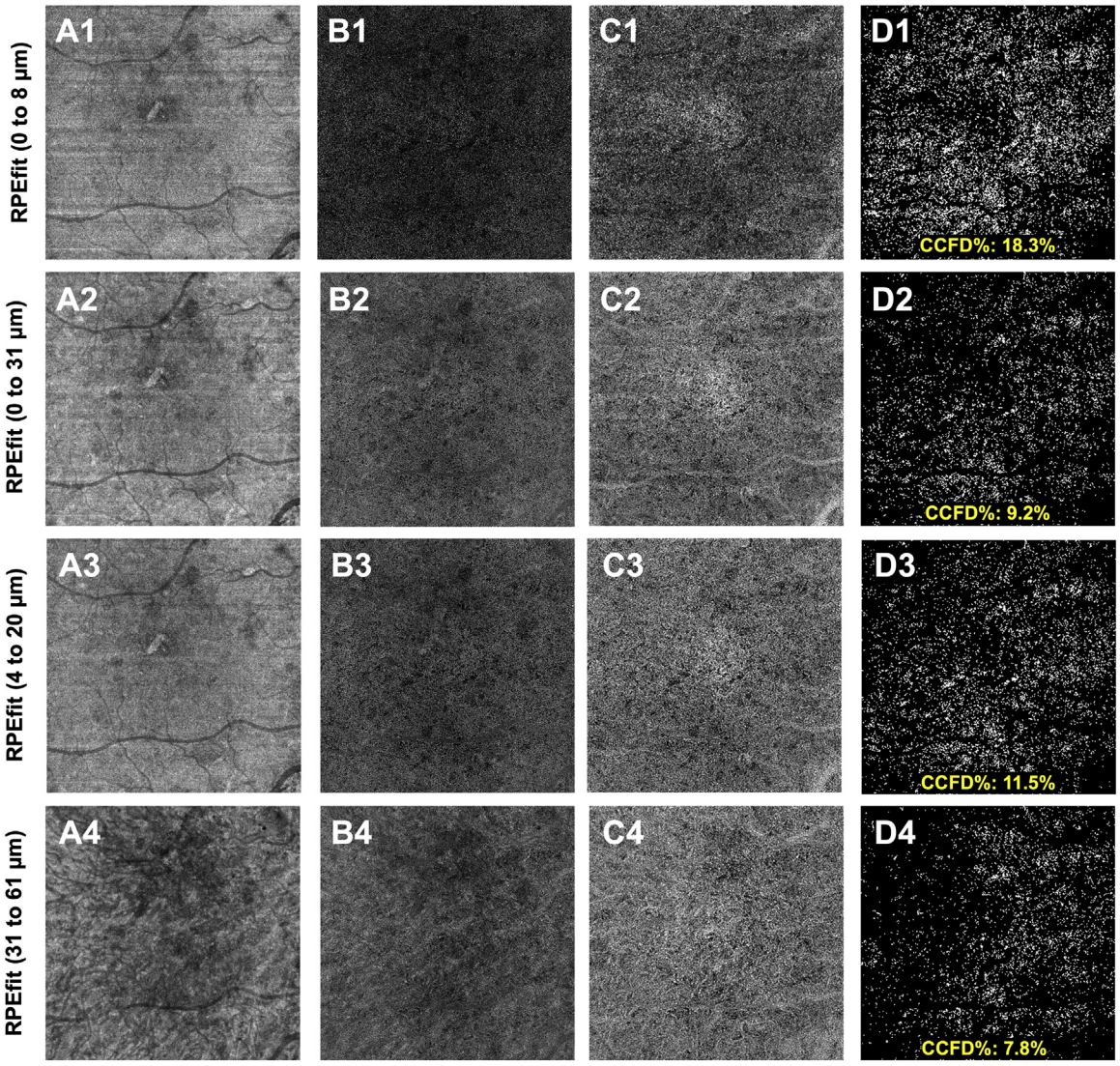

FIGURE 2. Compensation and binarization of choriocapillaris (CC) flow slabs from swept-source optical coherence tomography angiography (SS-OCTA) scans using 3 different slab boundaries. Row 1 (A1-D1): Slab boundaries set from the RPE fit to 8 µm below it. Row 2 (A2-D2): Slab boundaries set from the RPE fit to 31 µm below it. Row 3 (A3-D3): Slab boundaries set from 4 µm below the RPE fit to 20 µm below it. Row 4 (A4-D4): Slab boundaries set from 31 µm below the RPE fit to 61 µm below it. Column A (A1-A4): CC structural slabs. Column B (B1-B4): Uncompensated CC flow slabs. Column C (C1-C4): Compensated CC flow slabs. Column D (D1-D4): CC flow deficit (FD) binary maps generated from the compensated CC flow slabs. The choice of slab boundaries affects the appearance of the en face CC slabs and influences the computed CCFD%, highlighting the sensitivity of CC analysis to segmentation parameters. RPE = retinal pigment epithelium.

Among these 32 studies, 26 used SS-OCTA and 6 used SD-OCTA. The strategy has been validated on SS-OCTA and should work also on SD-OCTA, but it has not been validated yet.

Eighteen studies instead opted for the removal of drusen from the analyzed area using drusen masks or to only analyze areas not affected by drusen.

• **THRESHOLDING AND BINARIZATION:** Of the 102 studies, 87 conducted a quantitative assessment of CC flow, and 15 reported only qualitative analyses. Among the studies performing quantitative analyses, 8 used software provided by the device manufacturer, whereas the remaining 79 relied on external software. ImageJ was the most commonly used external software, used in 47 studies, followed by custom software in 28 studies. Other software solutions included Adobe Photoshop (3 studies) and Imagenet 6.0 (1 study).

Among the 15 studies that exclusively performed a qualitative assessment, the analyzed characteristics included the

presence of reduced flow signal, the presence of dark halo, and the presence of macular neovascularization including its area and morphology.

Sixty studies used a binarization process to obtain CC perfusion or nonperfusion metrics. Thirty-one studies used a local thresholding strategy, with the Phansalkar method being the most commonly used in 29 studies, followed by the Niblack method in 2 studies. Eighteen studies used a global thresholding approach, with 4 specifically using the Otsu method, 2 using MaxEntropy, 1 applying the Fuzzy C-means method, and 1 using an SD approach. Additionally, 2 studies compared the performance of the Phansalkar method and Fuzzy C-means on the same dataset of eyes. Finally, 10 studies did not report the thresholding method used.

Of the 29 studies using the Phansalkar thresholding method, 27 reported the radius used for the binarization process. The radius is typically reported in pixels, ranging from 1 to 15 pixels. However, the pixel dimension of CC flow images can vary across devices and may also change during image processing. Consequently, although a scan covers a fixed area of the macula (eg, 6×6 mm or 3×3 mm), the number of pixels in the image affects the physical size represented by each pixel, altering the area covered by a given radius.

For instance, a radius of 15 pixels corresponds to approximately 87.9 μm in a 6×6 mm scan with 1024×1024 pixels, 180 μm in a 6×6 mm scan with 500×500 pixels, and 43.94 μm in a 3×3 mm scan with 1024×1024 pixels. Reporting the radius solely in pixels without specifying the image dimensions is therefore insufficient to standardize comparisons across studies.

Among the 8 studies that reported the radius only in pixels, 7 used a radius of 15 pixels, and 1 used a radius of 5 pixels. For the studies reporting a 15-pixel radius, 5 used 6×6 mm scans, and 2 used a 3×3 mm scan. The single study using a 5-pixel radius analyzed a 6×6 mm scan. However, because of the lack of reported image dimensions, it was not possible to calculate the radii in micrometers for these studies.

For 20 studies, the radius in micrometers was either directly reported or calculable based on the reported image dimensions. For studies using 6×6 mm scans, the radii ranged from 18 μm to 152 μm. For studies using 3×3 mm scans, the radii ranged from 43.94 μm to 180 μm. Two studies used 4.4×4.4 mm scans, both using a radius of 43.94 μm. Additionally, one study compared results using different radii, ranging from 10 μm to 150 μm, for both 3×3 mm and 6×6 mm scans. Another study directly compared the outcomes of using a 43.94 μm radius versus an 87.9 μm radius for 6×6 mm scans.

• **PROJECTION ARTIFACT REMOVAL:** Because the presence of projection artifacts from overlying retinal vessels (or other superficial reflective pathology) can alter CC metrics quantification, the removal of this projection usually is performed by the device or in the postprocessing analysis. These algorithms are usually embedded in the OCTA device. However, in case of exporting the raw data, custom algorithms should be used to remove projections. Of the 90 studies performing quantitative analysis, 56 specifically mentioned the removal of projection artifacts using either built-in or custom software. For the remaining 32 studies, it was not possible to determine whether projection artifacts were removed or the strategy used to remove them.

• **METRICS:** Since the introduction of OCTA devices, numerous quantitative parameters have been introduced to represent CC perfusion or nonperfusion. Among these, CC FDs are the most widely used parameter to characterize areas of decreased perfusion. CC FDs are defined as regions of undetectable flow that are larger than the physiological flow voids normally present between capillaries. Alternative terms used to describe this metric include flow void, signal void, or inner-choroidal FDs, all of which represent the same concept.

Quantitative metrics related to CC FDs include CC FD percentage (CCFD%), which was assessed in 42 studies and is defined as the proportion of the total area occupied by CC FDs relative to the entire CC area in the analyzed scan. The average size or area of CC FDs was measured in 17 studies, and the number of CC FDs was evaluated in 10 studies. Six studies assessed the total area of flow voids, 1 study evaluated the number of CC FDs per mm², and 1 study analyzed the fractal dimension of CC FDs. Likewise, the percent nonperfused CC area, also referred to as the percent area of CC nonperfusion, was calculated as the ratio of pixels falling below the threshold (total area of signal voids) to the total number of pixels in the analyzed CC area in 7 studies.

A key consideration in CC FD analysis is whether physiological intercapillary flow voids were accounted for or excluded. Among the 42 studies that assessed CCFD%, 17 explicitly removed normal intercapillary spacing, with 16 applying a threshold of 24 μm (the estimated normal intercapillary distance) to exclude physiological voids,[112] whereas 1 study used a threshold of 172 μm² for removal.

In contrast to nonperfusion metrics, some studies quantified perfusion by evaluating the status of capillaries. Twenty studies measured the VD of the CC, and 3 studies assessed perfusion density or vessel perfusion, which is calculated as the skeletonized VD. One study also analyzed the diameter of CC vessels.

Other less commonly reported metrics included CC porosity, which was assessed in 1 study but lacked a clear definition. Another study evaluated the CC decorrelation signal index, defined as the average decorrelation value of all pixels in the upper outer ETDRS sector of the en face CC angiogram. The vascular/stromal ratio of the CC was reported in 1 study and was defined as the ratio of VD to stromal density (1 − VD).

Two studies introduced the concept of low perfusion area, defined as the area where capillary density fell below the

0.1 percentile threshold of the corresponding location in 40 normal healthy eyes. Focal perfusion loss was subsequently defined as the percentage of CC loss within the low perfusion area compared with normal controls.

Three qualitative studies evaluated the area of hypointense CC flow signals by visually comparing them with the surrounding regions, without relying on objective quantitative measurements.

DISCUSSION

This study systematically reviews the literature on the use of OCTA to investigate the CC in patients with AMD. A total of 102 studies were analyzed, underscoring the extensive research and strong interest in understanding CC perfusion in AMD. However, this review reveals considerable variability in the methodologies used to study the CC, including differences in OCTA technologies, slabs selected for CC visualization, binarization thresholds, strategies to address signal attenuation using structural information, and terminology used to define different metrics. This variability highlights the need for standardization in CC assessment methodologies to ensure consistency and reliability in future research.

One of the main contributors to heterogeneity in studies assessing the CC in patients with AMD was the OCTA technology used for imaging. Specifically, 52 studies (51%) used SD-OCTA devices to analyze the CC, 49 studies used SS-OCTA devices, and 1 study used both technologies. Notably, SD-OCTA systems may be less effective in visualizing the CC.[7,10] This limitation is primarily due to their use of a wavelength of approximately 840 nm, which increases the optical scattering at the RPE complex, and more so with the presence of drusen, leading to signal attenuation and shadowing artifacts that can affect analyses. In contrast, SS-OCTA systems offer enhanced sensitivity and use a longer wavelength, improving penetration of the RPE, reducing shadowing artifacts, and enabling a more accurate evaluation of the CC in eyes with AMD. Furthermore, SS-OCTA systems typically acquire images at a faster rate (100 000-400 000 A-scans per second) compared with SD-OCTA (70 000-100 000 A-scans per second), resulting in improved image quality through better decorrelation between sequential scans.[113] These technological advantages make SS-OCTA a superior choice for detailed and high-resolution imaging of the choroid, particularly in the context of AMD. The superiority of SS-OCTA for studying the CC beneath drusen was demonstrated by Lane and associates,[8] who conducted a comparative study of SS- and SD-OCTA systems to assess CC flow impairment in early and intermediate AMD. In this study, patients with drusen underwent imaging with both systems on the same day. Ambiguous CC dropout was defined as areas with low OCTA signals on en face CC images corresponding to low signals on en face structural OCT scans. The authors found that SS-OCTA was significantly less prone to generating false-positive flow impairment areas, underscoring its advantages in AMD imaging.

Additionally, another important limitation in comparing CC metrics across studies is the heterogeneity in OCTA scan sizes and scanning resolutions. Although 6×6 mm and 3×3 mm scans were the most commonly used, other scan dimensions were used less frequently, leading to inconsistencies in the field of view and image sampling. Additionally, scanning resolution varies between devices and scan protocols, with smaller scan sizes (eg, 3×3 mm) typically offering higher lateral resolution but covering a more limited area, whereas larger scans (eg, 6×6 mm or 8×8 mm) provide a broader view at the expense of reduced resolution. Differences in axial resolution, sampling density, and interpolation methods across SD- and SS-OCTA further contribute to variability in CC assessment. Standardized imaging protocols and reporting guidelines are needed to minimize these discrepancies and improve reproducibility in future research.

Although OCTA data are collected as volumetric data, the en face 2-dimensional visualization used for qualitative and quantitative assessment of the CC is typically created by defining an inner and outer boundary within the 3-dimensional OCTA cube. The flow data within these boundaries are projected to create the en face image. Currently, there is no clear consensus on the optimal boundaries or thickness of the CC slab. Ideally, the thickness of the CC slab should match the axial diameter of a single CC vessel, which decreases with age—from an average of 9.8 μm in the first decade of life to 6.5 μm in the tenth decade of life.[9] Because of the convolutional effects of OCT resolution, which artificially enlarge biological structures during imaging, a CC slab thickness of 10 to 20 μm has been suggested to be optimal.[11] This slab should be positioned in theory directly beneath the RPE/BM complex and shaped parallel to the hyperreflective line corresponding to this structure.[11]

Notably, the present study showed that the segmentation boundaries used to evaluate the CC varied significantly across the included studies, with marked discrepancies in the inner and outer boundaries, as well as in slab thickness. Our analysis showed that the CC slab thicknesses in the reviewed studies ranged from 4.4 μm to 30 μm. In most cases, the reference layer used to determine the inner and outer inferior boundaries comprised the RPE, RPE centerline, RPE fit, BM, and RPE-BM complex. However, these choices are not interchangeable for different reasons. First, the RPE thickness varies across the macula. When the RPE is used as the upper boundary with a fixed offset for the lower boundary, the slab's position relative to the CC can vary, even in normal eyes. This issue is further exacerbated in aging and AMD due to basal laminar deposits. Additionally, in the presence of drusen or RPE detachments, the RPE cannot be used as a reference to segment the CC and attempts to overcome this led to the use of the RPE fit defined

as a theoretical position of the RPE when no RPE detachment is present. Considering all these segmentation inconsistencies, BM is widely considered the preferred reference layer due to its stability. However, segmentation challenges and limited manufacturer support in past software versions have hindered its consistent use. Notably, no significant differences in segmentation approaches were found between SD- and SS-OCTA.

Notably, a substantial portion of studies (ie, 26 of 102) did not report segmentation boundaries, leading to uncertainty about the slabs used for CC visualization. It is important to note that an accurate CC slab is crucial for the compensation strategy (ie, see below), because slabs positioned deeper within the choroid may lead to variegated en face structural OCT images with brighter signals from choroidal pillars, vessels, and pigment in the deeper choroid. This can result in the introduction of artefacts when performing the compensation strategy.[114]

Previous studies examining the impact of slab position and thickness on CC quantitative metrics in both normal and GA eyes have shown that even minor positional shifts can lead to significant differences in quantitative CC measurement.[43,102] It was found that slabs positioned closer to BM were more prone to artifacts, such as regions of hypointensity, due to the inadvertent inclusion of the RPE layer caused by subtle segmentation errors. In contrast, deeper slabs demonstrated greater repeatability and were less affected by segmentation artifacts. However, deeper slabs may include signal contributions from structures located at those depths, introducing additional confounders. Of note, the optimal slab positioning is intrinsically tied to the nominal placement, accuracy, and robustness of the segmentation, because segmentation inconsistencies can exacerbate measurement variability and impact the reliability of CC metrics. Overall, variations in the CC slab position make it challenging to compare qualitative and quantitative CC data across different studies.

As mentioned above, to obtain the en face 2-dimensional visualization of the CC, a transverse slab is created within the 3-dimensional OCTA cube by defining an inner and outer boundary. Algorithms typically determine these boundaries by automatically detecting predefined macular layers based on characteristics such as reflectivity and texture. However, these segmentation algorithms generally are developed for healthy eyes and may fail in eyes with AMD. In such cases, reviewing the segmentation on the B-scans can reveal errors that require manual correction.

Notably, our systematic review found that only 61 studies reported manually adjusting the segmentation when the automated segmentation was found to be inaccurate. Even when manual corrections are performed, they are not straightforward, and their quality can vary significantly, potentially affecting the results. For instance, manual segmentations of BM under drusen often exhibit large variations across neighboring B-scans, introducing inconsistencies in the final CC analysis.

Averaging multiple en face OCTA images was shown to enhance the visualization of the CC. Uji and associates[115] demonstrated that this technique transforms the granular and often ambiguous appearance of single-frame SD-OCTA into a more coherent meshwork pattern, closely resembling histologic architecture. These findings may suggest that averaging can reduce noise and improve the accuracy of CC assessments, but also introduces the need to register images, which may also introduce variability, especially in eyes with AMD. However, as highlighted by Hiya and associates,[116] the test-retest variability of CCFD% in both intermediate AMD and GA eyes is low, with intraclass correlation coefficients of 0.98 and 0.96, respectively, within a 5-mm fovea-centered circle. These results suggest that single scans may already provide highly reproducible measurements, limiting the incremental value of averaging in certain clinical or research settings.

In AMD, the OCT and OCTA signals can be notably attenuated when passing through disease-related lesions, such as drusen. Although SS-OCTA provides improved penetration and signal detection in the presence of the RPE, signal attenuation beneath drusen still occurs.[67] This limitation in assessing the CC using OCTA in patients with AMD can be effectively addressed with a compensation strategy. Zhang and associates[40] developed this approach, designing an algorithm that uses an inverted structural image derived from the CC slab to enhance the intensity of the CC flow image. This strategy also compensates for the lack of uniformity in the OCT signal across the scan area. Several studies have validated the compensation strategy,[11,67,101,117] but it does have limitations. Notably, it cannot address the presence of hyperreflective foci or calcified drusen, which result in complete signal loss that compensation strategies are unable to resolve.[11,12,101,118-120] Despite these limitations, the compensation strategy can enhance the qualitative and quantitative assessment of the CC on OCTA. However, our analysis revealed that this approach was used in only 33 of 102 studies.

Of the 102 studies included in our analysis, 87 conducted a quantitative assessment of CC flow, and 15 reported only qualitative analyses. To provide quantitative metrics of the CC, OCTA en face images are processed with a threshold that is applied to create binary images—in which pixels with a grayscale value above the applied threshold are displayed as white (or black) and pixels falling under the threshold are displayed as black (or white, respectively)—from grayscale images. In general, 3 different methodologies may be used to binarize OCTA images, as (1) "global" thresholding, (2) "local" thresholding, and (3) "complex" thresholding, in which binarization is obtained using both global and local thresholding algorithms. Of note, although a global threshold applies the same threshold value across the entire image, local (or adaptive) algorithms adapt threshold values to different regions of the image.[45] In the assessment of the CC in AMD, a local thresholding might be considered as a preferable methodology to

binarize images because it accounts for regional differences in image brightness. However, only 31 studies used a local thresholding strategy, with the Phansalkar method being the most commonly used. Several significant studies have suggested that the latter thresholding strategy may be the most effective approach for assessing the CC in patients with AMD.[11,117]

When using a local threshold, a critical factor influencing the final binarized image is the radius applied. The radius defines the size of the neighborhood area of pixels considered by the algorithm when determining whether a specific pixel falls above or below the threshold. When determining the radius, it is essential to consider the size of the pixels comprising the image, because the same radius can correspond to different neighborhood areas in images with varying dimensions and pixel densities. Among the analyzed studies, 27 of 29 studies using the Phansalkar thresholding method reported the radius size used, but 8 of these provided the radius in pixels without specifying the scan size or the pixel density—a key detail for determining the actual area. Regardless of the level of detail provided, the radius size varied significantly across the studies, even when the same image size was used, further underscoring the heterogeneity of the methodologies used.

Since the introduction of OCTA devices, various quantitative parameters have been developed to assess CC perfusion or nonperfusion. Among these, CC FDs are the most widely used metric to characterize areas of nonperfusion. CC FDs are defined as regions of nondetectable flow that exceed the size of the physiological flow voids typically found between capillaries. As such, Zhang and associates[112] have recommended applying a size threshold, such as removing FDs $\leq$24 μm, to mitigate the impact of speckle noise and enhance the reliability of CC quantification. Alternative terms for this metric include flow voids, signal voids, or inner-choroid FDs, all of which refer to the same concept. Less commonly, some studies assessed CC perfusion by measuring perfused areas rather than areas of nonperfusion. This approach underscores the heterogeneity in the metrics used to evaluate the CC, which complicates comparisons between different studies.

Although recent guidelines have offered valuable recommendations for general CC imaging, particularly in terms of segmentation strategies, preferred metrics such as CCFD%, and thresholding approaches, they fall short in addressing the unique challenges posed by AMD.[11] Notably, there is a lack of guidance on selecting appropriate compensation strategies and evaluating their case-by-case adequacy in AMD eyes. Certain disease-specific features, such as hyperreflective foci and calcified drusen that are known to significantly attenuate or block the OCT signal, will prevent the accurate assessment of the underlying CC on OCTA.[12,118,121] These lesions need to be excluded from the CC assessment. In addition, a tailored approach is needed to differentiate cases where compensation is necessary, such as in eyes with drusen, from those where it may be inappropriate or even misleading, as in eyes with GA.[122] As such, future standardization efforts must extend beyond general imaging protocols and incorporate AMD-specific and instrument-specific considerations.[122] Only through such targeted and AMD-specific strategies can reproducibility and clinical applicability of CC imaging in AMD be reliably achieved.

In conclusion, this study revealed substantial heterogeneity in the methodologies used to investigate the CC in AMD. This variability encompassed differences in OCTA technologies, slab selection for CC visualization, binarization thresholds, and approaches to address signal attenuation using structural information. Although guidelines for CC assessment have been published,[11] our findings underscore the critical need for further standardization of methodologies to enhance consistency and reliability in future research.

CREDIT AUTHORSHIP CONTRIBUTION STATEMENT

Alessandro Berni: Writing – review & editing, Writing – original draft, Methodology, Formal analysis, Data curation, Conceptualization. **Claudio Foti:** Writing – review & editing, Methodology, Data curation, Conceptualization. **Lorena Ulla:** Writing – review & editing, Formal analysis, Data curation. **Chinmayi Vyas:** Writing – review & editing, Formal analysis, Data curation. **Jay Chhablani:** Writing – review & editing, Validation. **Varun Chaudhary:** Writing – review & editing, Validation. **Yousif Subhi:** Writing – review & editing, Validation. **Giovanni Gregori:** Writing – review & editing, Validation. **Ruikang K. Wang:** Writing – review & editing, Validation. **Philip J. Rosenfeld:** Writing – review & editing, Validation. **SriniVas R. Sadda:** Writing – review & editing, Validation. **Francesco Bandello:** Writing – review & editing, Validation. **Michele Reibaldi:** Writing – review & editing, Validation, Project administration, Methodology, Conceptualization. **Enrico Borrelli:** Writing – review & editing, Writing – original draft, Validation, Supervision, Resources, Project administration, Methodology, Investigation, Funding acquisition, Formal analysis, Data curation, Conceptualization.

Acknowledgments:
This study received no funding. Financial Disclosures: Dr Chhablani reports the following disclosures: Netramind Innovations (O), Erasca (C), Allergan (C), and Bausch & Lomb (C). Dr Chaudhary reports acting as an advisory board member, grants and other from Novartis; acting as an advisory board member, grants and other from Bayer; grants from Allergan; acting as an advisory board member and grants from Roche; acting as an advisory board member for Janssen; acting as an advisory board member for Apellis; and acting as an advisory board member for Boehringer Ingelheim outside the submitted work. Drs Gregori and Rosenfeld received research support from Carl Zeiss Meditec, Inc. Dr Gregori and the University of Miami co-own a patent that is licensed to Carl Zeiss Meditec, Inc. Dr Rosenfeld also received research funding from Gyroscope Therapeutics. He is also a consultant for AbbVie, Apellis, Bayer Pharmaceuticals, Boehringer-Ingelheim, Carl Zeiss Meditec, Genentech/Roche, InflammX Therapeutics, Ocudyne, Regeneron 47 Pharmaceuticals, and Unity Biotechnology. He also has equity interest in Apellis, InflammX, Ocudyne, and Valitor. Dr Wang received financial support from Colgate Palmolive Company and Estee Lauder lnc, and is a consultant for Carl Zeiss Meditec and Cyberdontics. He also has several patents: US8, 750, 586, US8, 180, 134, US9, 282,905, US9, 759,544, US10, 354, 378, US10, 529,061. Dr Sadda reports consultancy for 4DMT, Alexion, Allergan, Alnylam Pharmaceuticals; Amgen, Apellis Pharmaceuticals, Astellas, Bayer Healthcare Pharmaceuticals, Biogen, Boehringer Ingelheim, Carl Zeiss Meditec, Catalyst Pharmaceuticals, Centervue, Roche/Genentech, Gyroscope Therapeutics, Heidelberg Engineering, Iveric Bio, Janssen Pharmaceuticals, Merck & Co, Nanoscope, Novartis, Optos, Oxurion/Thrombogenics, Pfizer, Regeneron Pharmaceuticals, Samsung Bioepis, and Vertex Pharmaceuticals. He reports lecture fees from Carl Zeiss Meditec, Heidelberg Engineering, Nidek, Novartis, and Topcon Medical Systems Inc. He also has received research grant support from Carl Zeiss Meditec and Research Instruments from Carl Zeiss Meditec, Heidelberg Engineering, Nidek Incorporated, Optos, and Centervue. Dr Reibaldi is a consultant for AbbVie, Bayer, Roche, and Novartis. Dr Borrelli is a consultant for AbbVie, Bayer, Hofmann La Roche, and Zeiss. All authors attest that they meet the current ICMJE criteria for authorship. Author Contributions: Study concept and design: A.B., C.F., M.R., and E.B. Acquisition, analysis, or interpretation of data: All authors. Drafting of the manuscript: A.B. and E.B. Critical revision of the manuscript for important intellectual content: All authors. Statistical analysis: A.B. Study supervision: E.B.
Financial Disclosures: The authors declare that they have no known competing financial interests or personal relationships that could have appeared to influence the work reported in this paper.

REFERENCES

1. Ferris 3rd FL, Wilkinson CP, Bird A, et al. Clinical classification of age-related macular degeneration. *Ophthalmology*. 2013;120(4):844–851. doi:10.1016/j.ophtha.2012.10.036.
2. Klein R, Klein BEK, Linton KLP. Prevalence of age-related maculopathy: The Beaver Dam Eye Study. *Ophthalmology*. 2020;127(4S):S122–S132. doi:10.1016/j.ophtha.2020.01.033.
3. Wong WL, Su X, Li X, et al. Global prevalence of age-related macular degeneration and disease burden projection for 2020 and 2040: a systematic review and meta-analysis. *Lancet Glob Health*. 2014;2(2):e106–e116. doi:10.1016/S2214-109X(13)70145-1.
4. Borrelli E, Reibaldi M, Bandello F, Lanzetta P, Boscia F. Ensuring the strict and accurate adherence to inclusion criteria in clinical trials for AMD is crucial. *Eye (Lond)*. 2024;38(16):3037–3038. doi:10.1038/s41433-024-03232-9.
5. Dolz-Marco R, Balaratnasingam C, Messinger JD, et al. The border of macular atrophy in age-related macular degeneration: a clinicopathologic correlation. *Am J Ophthalmol*. 2018;193:166–177. doi:10.1016/j.ajo.2018.06.020.
6. Fleckenstein M, Keenan TDL, Guymer RH, et al. Age-related macular degeneration. *Nat Rev Dis Primers*. 2021;7(1):31. doi:10.1038/s41572-021-00265-2.
7. Borrelli E, Sarraf D, Freund KB, Sadda SR. OCT angiography and evaluation of the choroid and choroidal vascular disorders. *Prog Retin Eye Res*. 2018;67:30–55. doi:10.1016/j.preteyeres.2018.07.002.
8. Lane M, Moult EM, Novais EA, et al. Visualizing the choriocapillaris under drusen: comparing 1050-nm swept-source versus 840-nm spectral-domain optical coherence tomography angiography. *Invest Ophthalmol Vis Sci*. 2016;57(9):585–590 JOCT. doi:10.1167/iovs.15-18915.
9. Ramrattan RS, van der Schaft TL, Mooy CM, de Bruijn WC, Mulder PG, de Jong PT. Morphometric analysis of Bruch's membrane, the choriocapillaris, and the choroid in aging. *Invest Ophthalmol Vis Sci*. 1994;35(6):2857–2864.
10. Spaide RF, Fujimoto JG, Waheed NK, Sadda SR, Staurenghi G. Optical coherence tomography angiography. *Prog Retin Eye Res*. 2018;64:1–55. doi:10.1016/j.preteyeres.2017.11.003.
11. Chu Z, Zhang Q, Gregori G, Rosenfeld PJ, Wang RK. Guidelines for imaging the choriocapillaris using OCT angiography. *Am J Ophthalmol*. 2021;222:92–101. doi:10.1016/j.ajo.2020.08.045.
12. Cheng Y, Hiya F, Li J, et al. Calcified drusen prevent the detection of underlying choriocapillaris using swept-source optical coherence tomography angiography. *Invest Ophthalmol Vis Sci*. 2024;65(6):26. doi:10.1167/iovs.65.6.26.
13. Moult E, Choi W, Waheed NK, et al. Ultrahigh-speed swept-source OCT angiography in exudative AMD. *Ophthalmic Surg Lasers Imaging Retina*. 2014;45(6):496–505. doi:10.3928/23258160-20141118-03.
14. Choi W, Moult EM, Waheed NK, et al. Ultrahigh-speed, swept-source optical coherence tomography angiography in nonexudative age-related macular degeneration with geographic atrophy. *Ophthalmology*. 2015;122(12):2532–2544. doi:10.1016/j.ophtha.2015.08.029.
15. El Ameen A, Cohen SY, Semoun O, et al. Type 2 neovascularization secondary to age-related macular degeneration imaged by optical coherence tomography angiography. *Retina*. 2015;35(11):2212–2218. doi:10.1097/IAE.0000000000000773.
16. Miere A, Querques G, Semoun O, El Ameen A, Capuano V, Souied EH. Optical coherence tomography angiography in early type 3 neovascularization. *Retina*. 2015;35(11):2236–2241. doi:10.1097/IAE.0000000000000834.
17. Miere A, Semoun O, Cohen SY, et al. Optical coherence tomography angiography features of subretinal fibrosis in age-related macular degeneration. *Retina*. 2015;35(11):2275–2284. doi:10.1097/IAE.0000000000000819.
18. Alten F, Heiduschka P, Clemens CR, Eter N. Exploring choriocapillaris under reticular pseudodrusen using OCT-angiography. *Graefes Arch Clin Exp Ophthalmol*. 2016;254(11):2165–2173. doi:10.1007/s00417-016-3375-1.

19. Pellegrini M, Acquistapace A, Oldani M, et al. Dark atrophy: an optical coherence tomography angiography study. *Ophthalmology*. 2016;123(9):1879–1886. doi:10.1016/j.ophtha.2016.05.041.
20. Spaide RF. Choriocapillaris flow features follow a power law distribution: implications for characterization and mechanisms of disease progression. *Am J Ophthalmol*. 2016;170:58–67. doi:10.1016/j.ajo.2016.07.023.
21. Alten F, Lauermann JL, Clemens CR, Heiduschka P, Eter N. Signal reduction in choriocapillaris and segmentation errors in spectral domain OCT angiography caused by soft drusen. *Graefes Arch Clin Exp Ophthalmol*. 2017;255(12):2347–2355. doi:10.1007/s00417-017-3813-8.
22. Borrelli E, Uji A, Sarraf D, Sadda SR. Alterations in the choriocapillaris in intermediate age-related macular degeneration. *Invest Ophthalmol Vis Sci*. 2017;58(11):4792–4798. doi:10.1167/iovs.17-22360.
23. Cicinelli MV, Rabiolo A, Marchese A, et al. Choroid morphometric analysis in non-neovascular age-related macular degeneration by means of optical coherence tomography angiography. *Br J Ophthalmol*. 2017;101(9):1193–1200. doi:10.1136/bjophthalmol-2016-309481.
24. Kvanta A, Casselholm de Salles M, Amren U, Bartuma H. Optical coherence tomography angiography of the foveal microvasculature in geographic atrophy. *Retina*. 2017;37(5):936–942. doi:10.1097/IAE.0000000000001248.
25. Miere A, Querques G, Semoun O, et al. Optical coherence tomography angiography changes in early type 3 neovascularization after anti-vascular endothelial growth factor treatment. *Retina*. 2017;37(10):1873–1879. doi:10.1097/IAE.0000000000001447.
26. Nesper PL, Soetikno BT, Fawzi AA. Choriocapillaris nonperfusion is associated with poor visual acuity in eyes with reticular pseudodrusen. *Am J Ophthalmol*. 2017;174:42–55. doi:10.1016/j.ajo.2016.10.005.
27. Borrelli E, Mastropasqua R, Senatore A, et al. Impact of choriocapillaris flow on multifocal electroretinography in intermediate age-related macular degeneration eyes. *Invest Ophthalmol Vis Sci*. 2018;59(4):AMD25–AMD30. doi:10.1167/iovs.18-23943.
28. Borrelli E, Shi Y, Uji A, et al. Topographic analysis of the choriocapillaris in intermediate age-related macular degeneration. *Am J Ophthalmol*. 2018;196:34–43. doi:10.1016/j.ajo.2018.08.014.
29. Borrelli E, Souied EH, Freund KB, et al. Reduced choriocapillaris flow in eyes with type 3 neovascularization and age-related macular degeneration. *Retina*. 2018;38(10):1968–1976. doi:10.1097/IAE.0000000000002198.
30. Chatziralli I, Theodossiadis G, Panagiotidis D, Pousoulidi P, Theodossiadis P. Choriocapillaris vascular density changes in patients with drusen: cross-sectional study based on optical coherence tomography angiography findings. *Ophthalmol Ther*. 2018;7(1):101–107. doi:10.1007/s40123-018-0119-9.
31. Chatziralli I, Theodossiadis G, Panagiotidis D, Pousoulidi P, Theodossiadis P. Choriocapillaris' alterations in the presence of reticular pseudodrusen compared to drusen: study based on OCTA findings. *Int Ophthalmol*. 2018;38(5):1887–1893. doi:10.1007/s10792-017-0671-7.
32. Lee B, Ahn J, Yun C, Kim SW, Oh J. Variation of retinal and choroidal vasculatures in patients with age-related macular degeneration. *Invest Ophthalmol Vis Sci*. 2018;59(12):5246–5255. doi:10.1167/iovs.17-23600.
33. Martins A, Farinha C, Raimundo M, et al. Multimodal evaluation of the fellow eye of patients with retinal angiomatous proliferation. *Ophthalmic Res*. 2018;59(2):88–97. doi:10.1159/000481262.
34. Muller PL, Pfau M, Moller PT, et al. Choroidal flow signal in late-onset Stargardt disease and age-related macular degeneration: an OCT-angiography study. *Invest Ophthalmol Vis Sci*. 2018;59(4):AMD122–AMD131. doi:10.1167/iovs.18-23819.
35. Nesper PL, Lutty GA, Fawzi AA. Residual choroidal vessels in atrophy can masquerade as choroidal neovascularization on optical coherence tomography angiography: introducing a clinical and software approach. *Retina*. 2018;38(7):1289–1300. doi:10.1097/IAE.0000000000001863.
36. Qin J, Rinella N, Zhang Q, et al. OCT Angiography and cone photoreceptor imaging in geographic atrophy. *Invest Ophthalmol Vis Sci*. 2018;59(15):5985–5992. doi:10.1167/iovs.18-25032.
37. Rispoli M, Savastano MC, Lumbroso B. Quantitative vascular density changes in choriocapillaris around CNV after anti-VEGF treatment: dark halo. *Ophthalmic Surg Lasers Imaging Retina*. 2018;49(12):918–924. doi:10.3928/23258160-20181203-02.
38. Sacconi R, Corbelli E, Carnevali A, Querques L, Bandello F, Querques G. Optical coherence tomography angiography in geographic atrophy. *Retina*. 2018;38(12):2350–2355. doi:10.1097/IAE.0000000000001873.
39. Treister AD, Nesper PL, Fayed AE, Gill MK, Mirza RG, Fawzi AA. Prevalence of subclinical CNV and choriocapillaris nonperfusion in fellow eyes of unilateral exudative AMD on OCT angiography. *Transl Vis Sci Technol*. 2018;7(5):19. doi:10.1167/tvst.7.5.19.
40. Zhang Q, Zheng F, Motulsky EH, et al. A novel strategy for quantifying choriocapillaris flow voids using swept-source OCT angiography. *Invest Ophthalmol Vis Sci*. 2018;59(1):203–211. doi:10.1167/iovs.17-22953.
41. Alagorie AR, Verma A, Nassisi M, Sadda SR. Quantitative assessment of choriocapillaris flow deficits in eyes with advanced age-related macular degeneration versus healthy eyes. *Am J Ophthalmol*. 2019;205:132–139. doi:10.1016/j.ajo.2019.04.037.
42. Braun PX, Mehta N, Gendelman I, et al. Global analysis of macular choriocapillaris perfusion in dry age-related macular degeneration using swept-source optical coherence tomography angiography. *Invest Ophthalmol Vis Sci*. 2019;60(15):4985–4990. doi:10.1167/iovs.19-27861.
43. Byon I, Nassisi M, Borrelli E, Sadda SR. Impact of slab selection on quantification of choriocapillaris flow deficits by optical coherence tomography angiography. *Am J Ophthalmol*. 2019;208:397–405. doi:10.1016/j.ajo.2019.08.026.
44. Camino A, Guo Y, You Q, et al. Detecting and measuring areas of choriocapillaris low perfusion in intermediate, non-neovascular age-related macular degeneration. *Neurophotonics*. 2019;6(4):041108. doi:10.1117/1.NPh.6.4.041108.
45. Chu Z, Gregori G, Rosenfeld PJ, Wang RK. Quantification of choriocapillaris with optical coherence tomography angiography: a comparison study. *Am J Ophthalmol*. 2019;208:111–123. doi:10.1016/j.ajo.2019.07.003.

46. Emre S, Ulusoy MO. Optical coherence tomography angiography findings of the fellow eye of patients with unilateral neovascular age-related macular degeneration OCT-A evaluation of fellow eyes of CNV. *Rom J Ophthalmol*. 2019;63(3):231–237.
47. Heiferman MJ, Fawzi AA. Progression of subclinical choroidal neovascularization in age-related macular degeneration. *PLoS One*. 2019;14(6):e0217805. doi:10.1371/journal.pone.0217805.
48. Hikichi T, Agarie M. Reduced vessel density of the choriocapillaris during anti-vascular endothelial growth factor therapy for neovascular age-related macular degeneration. *Invest Ophthalmol Vis Sci*. 2019;60(4):1088–1095. doi:10.1167/iovs.18-24522.
49. Hou KK, Au A, Kashani AH, Freund KB, Sadda SR, Sarraf D. Pseudoflow with OCT angiography in eyes with hard exudates and macular drusen. *Transl Vis Sci Technol*. 2019;8(3):50. doi:10.1167/tvst.8.3.50.
50. Keiner CM, Zhou H, Zhang Q, et al. Quantifying choriocapillaris hypoperfusion in patients with choroidal neovascularization using swept-source OCT angiography. *Clin Ophthalmol*. 2019;13:1613–1620. doi:10.2147/OPTH.S204344.
51. Lee B, Yoo G, Yun C, Oh J. Short-term effects of anti-vascular endothelial growth factor on peripapillary choroid and choriocapillaris in eyes with neovascular age-related macular degeneration. *Graefes Arch Clin Exp Ophthalmol*. 2019;257(10):2163–2172. doi:10.1007/s00417-019-04432-w.
52. Nassisi M, Baghdasaryan E, Borrelli E, Ip M, Sadda SR. Choriocapillaris flow impairment surrounding geographic atrophy correlates with disease progression. *PLoS One*. 2019;14(2):e0212563. doi:10.1371/journal.pone.0212563.
53. Nassisi M, Shi Y, Fan W, et al. Choriocapillaris impairment around the atrophic lesions in patients with geographic atrophy: a swept-source optical coherence tomography angiography study. *Br J Ophthalmol*. 2019;103(7):911–917. doi:10.1136/bjophthalmol-2018-312643.
54. Nassisi M, Tepelus T, Nittala MG, Sadda SR. Choriocapillaris flow impairment predicts the development and enlargement of drusen. *Graefes Arch Clin Exp Ophthalmol*. 2019;257(10):2079–2085. doi:10.1007/s00417-019-04403-1.
55. Rinella NT, Zhou H, Zhang Q, et al. Quantifying choriocapillaris flow voids in patients with geographic atrophy using swept-source OCT angiography. *Ophthalmic Surg Lasers Imaging Retina*. 2019;50(9):e229–e235. doi:10.3928/23258160-20190905-14.
56. Streho M, Lavallee G, Aimadaly M, et al. Geographic atrophy and OCT angiography: descriptive study and correlation with autofluorescence. *Ophthalmic Surg Lasers Imaging Retina*. 2019;50(9):e222–e228. doi:10.3928/23258160-20190905-13.
57. Takasago Y, Shiragami C, Kobayashi M, et al. Macular atrophy findings by optical coherence tomography angiography compared with fundus autofluorescence in treated exudative age-related macular degeneration. *Retina*. 2019;39(2):296–302. doi:10.1097/IAE.0000000000001980.
58. Thulliez M, Zhang Q, Shi Y, et al. Correlations between choriocapillaris flow deficits around geographic atrophy and enlargement rates based on swept-source OCT imaging. *Ophthalmol Retina*. 2019;3(6):478–488. doi:10.1016/j.oret.2019.01.024.
59. Vujosevic S, Toma C, Villani E, et al. Quantitative choriocapillaris evaluation in intermediate age-related macular degeneration by swept-source optical coherence tomography angiography. *Acta Ophthalmol*. 2019;97(6):e919–e926. doi:10.1111/aos.14088.
60. Alagorie AR, Verma A, Nassisi M, et al. Quantitative assessment of choriocapillaris flow deficits surrounding choroidal neovascular membranes. *Retina*. 2020;40(11):2106–2112. doi:10.1097/IAE.0000000000002878.
61. Borrelli E, Sacconi R, Zuccaro B, et al. Photoreceptor alteration in intermediate age-related macular degeneration. *Sci Rep*. 2020;10(1):21036. doi:10.1038/s41598-020-78201-9.
62. Cennamo G, Montorio D, D'Alessandro A, Napolitano P, D'Andrea L, Tranfa F. Prospective study of vessel density by optical coherence tomography angiography after intravitreal bevacizumab in exudative age-related macular degeneration. *Ophthalmol Ther*. 2020;9(1):77–85. doi:10.1007/s40123-019-00221-0.
63. Hecht A, Pollreisz A, Sayegh R, et al. Relationship between morphological and vascular alterations in geographic atrophy using a multimodal imaging approach. *Acta Ophthalmol*. 2020;98(6):e700–e708. doi:10.1111/aos.14352.
64. Luo M, Zhao X, Zhao N, et al. Comparison of choriocapillary flow density between fellow eyes of polypoidal choroidal vasculopathy and neovascular age-related macular degeneration. *BMC Ophthalmol*. 2020;20(1):162. doi:10.1186/s12886-020-01386-0.
65. Moult EM, Alibhai AY, Rebhun C, et al. Spatial distribution of choriocapillaris impairment in eyes with choroidal neovascularization secondary to age-related macular degeneration: a quantitative OCT Angiography study. *Retina*. 2020;40(3):428–445. doi:10.1097/IAE.0000000000002556.
66. Parisi V, Ziccardi L, Costanzo E, et al. Macular functional and morphological changes in intermediate age-related maculopathy. *Invest Ophthalmol Vis Sci*. 2020;61(5):11. doi:10.1167/iovs.61.5.11.
67. Shi Y, Chu Z, Wang L, et al. Validation of a compensation strategy used to detect choriocapillaris flow deficits under drusen with swept source OCT angiography. *Am J Ophthalmol*. 2020;220:115–127. doi:10.1016/j.ajo.2020.06.033.
68. Tiosano L, Byon I, Alagorie AR, Ji YS, Sadda SR. Choriocapillaris flow deficit associated with intraretinal hyperreflective foci in intermediate age-related macular degeneration. *Graefes Arch Clin Exp Ophthalmol*. 2020;258(11):2353–2362. doi:10.1007/s00417-020-04837-y.
69. Vaghefi E, Hill S, Kersten HM, Squirrell D. Quantification of optical coherence tomography angiography in age and age-related macular degeneration using vessel density analysis. *Asia Pac J Ophthalmol (Phila)*. 2020;9(2):137–143. doi:10.1097/APO.0000000000000278.
70. Yuan MZ, Chen LL, Yang JY, Luo MY, Chen YX. Comparison of OCT and OCTA manifestations among untreated PCV, neovascular AMD, and CSC in Chinese population. *Int J Ophthalmol*. 2020;13(1):93–103. doi:10.18240/ijo.2020.01.14.
71. Clemens CR, Lauermann JL, Schmitz B, Eter N, Alten F. Longitudinal choriocapillaris changes in the presence of reticular pseudodrusen. *Sci Rep*. 2021;11(1):18227. doi:10.1038/s41598-021-97771-w.

72. Corvi F, Cozzi M, Corradetti G, Staurenghi G, Sarraf D, Sadda SR. Quantitative assessment of choriocapillaris flow deficits in eyes with macular neovascularization. *Graefes Arch Clin Exp Ophthalmol*. 2021;259(7):1811–1819. doi:10.1007/s00417-020-05056-1.
73. Corvi F, Tiosano L, Corradetti G, et al. Choriocapillaris flow deficits as a risk factor for progression of age-related macular degeneration. *Retina*. 2021;41(4):686–693. doi:10.1097/IAE.0000000000002990.
74. Hacker V, Reiter GS, Schranz M, et al. Impact of large choroidal vessels on choriocapillaris flow deficit analyses in optical coherence tomography angiography. *PLoS One*. 2021;16(8):e0254955. doi:10.1371/journal.pone.0254955.
75. Khorrami Kashi A, Souied E, Fares S, et al. The spectrum of central choriocapillaris abnormalities on swept-source optical coherence tomography angiography in the fellow eye of unilateral exudative age-related macular degeneration patients: from flow deficits to subclinical non-exudative neovascularization. *J Clin Med*. 2021;10(12):2658. doi:10.3390/jcm10122658.
76. Lee H, Kim S, Kim MA, et al. Integrative analysis of the choroid by quantifying Haller vessel and choriocapillaris parameters in different drusen subtypes. *Sci Rep*. 2021;11(1):15509. doi:10.1038/s41598-021-94627-1.
77. Montorio D, D'Andrea L, Mirto N, Cennamo G. The role of optical coherence tomography angiography in reticular pseudodrusen. *Photodiagnosis Photodyn Ther*. 2021;33:102094. doi:10.1016/j.pdpdt.2020.102094.
78. Moult EM, Shi Y, Zhang Q, et al. Analysis of correlations between local geographic atrophy growth rates and local OCT angiography-measured choriocapillaris flow deficits. *Biomed Opt Express*. 2021;12(7):4573–4595. doi:10.1364/BOE.427819.
79. Nassisi M, Tepelus T, Corradetti G, Sadda SR. Relationship between choriocapillaris flow and scotopic microperimetry in early and intermediate age-related macular degeneration. *Am J Ophthalmol*. 2021;222:302–309. doi:10.1016/j.ajo.2020.04.018.
80. Rosa R, Corazza P, Musolino M, et al. Choroidal changes in intermediate age-related macular degeneration patients with drusen or pseudodrusen. *Eur J Ophthalmol*. 2021;31(2):505–513. doi:10.1177/1120672120914530.
81. Sacconi R, Corbelli E, Borrelli E, et al. Choriocapillaris flow impairment could predict the enlargement of geographic atrophy lesion. *Br J Ophthalmol*. 2021;105(1):97–102. doi:10.1136/bjophthalmol-2019-315800.
82. Savastano MC, Rizzo C, Gambini G, et al. Choriocapillaris vascular density changes: healthy vs. advanced exudative age-related macular degeneration previously treated with multiple anti-VEGF intravitreal injections. *Diagnostics (Basel)*. 2021;11(11):1958. doi:10.3390/diagnostics11111958.
83. Shen M, Zhang Q, Yang J, et al. Swept-source OCT angiographic characteristics of treatment-naive nonexudative macular neovascularization in AMD prior to exudation. *Invest Ophthalmol Vis Sci*. 2021;62(6):14. doi:10.1167/iovs.62.6.14.
84. Temel E, Batioglu F, Demirel S, Ozcan G, Yanik O, Ozmert E. Vascular and structural alterations of the choroid evaluated by optical coherence tomography angiography and enhanced-depth imaging optical coherence tomography in eyes with reticular pseudodrusen and soft drusen. *Photodiagnosis Photodyn Ther*. 2021;36:102549. doi:10.1016/j.pdpdt.2021.102549.
85. Tiosano L, Corradetti G, Sadda SR. Progression of choriocapillaris flow deficits in clinically stable intermediate age-related macular degeneration. *Eye (Lond)*. 2021;35(11):2991–2998. doi:10.1038/s41433-020-01298-9.
86. You QS, Camino A, Wang J, et al. Geographic atrophy progression is associated with choriocapillaris flow deficits measured with optical coherence tomographic angiography. *Invest Ophthalmol Vis Sci*. 2021;62(15):28. doi:10.1167/iovs.62.15.28.
87. Arrigo A, Amato A, Barresi C, et al. Choroidal modifications preceding the onset of macular neovascularization in age-related macular degeneration. *Ophthalmol Ther*. 2022;11(1):377–386. doi:10.1007/s40123-021-00443-1.
88. Harada N, Nagai N, Mushiga Y, Ozawa Y. Choriocapillaris flow imbalance in fellow eyes in age-related macular degeneration. *Invest Ophthalmol Vis Sci*. 2022;63(9):13. doi:10.1167/iovs.63.9.13.
89. Rinella NT, Zhou H, Wong J, et al. Correlation between localized choriocapillaris perfusion and macular function in eyes with geographic atrophy. *Am J Ophthalmol*. 2022;234:174–182. doi:10.1016/j.ajo.2021.08.007.
90. Savastano MC, Fossataro C, Carla MM, et al. OCT angiography analysis of choriocapillaris vascular density in different stages of age-related macular degeneration. *Front Ophthalmol (Lausanne)*. 2022;2:985262. doi:10.3389/fopht.2022.985262.
91. Viggiano P, Grassi MO, Pignataro M, et al. Topographical analysis of the choriocapillaris reperfusion after loading anti-VEGF therapy in neovascular AMD. *Transl Vis Sci Technol*. 2022;11(9):18. doi:10.1167/tvst.11.9.18.
92. Wu Z, Zhou X, Chu Z, et al. Impact of reticular pseudodrusen on choriocapillaris flow deficits and choroidal structure on optical coherence tomography angiography. *Invest Ophthalmol Vis Sci*. 2022;63(12):1. doi:10.1167/iovs.63.12.1.
93. Cabral D, Fradinho AC, Zhang Y, et al. Quantitative assessment of choriocapillaris flow deficits and type 1 macular neovascularization growth in age-related macular degeneration. *Sci Rep*. 2023;13(1):8572. doi:10.1038/s41598-023-35080-0.
94. Ersoz MG, Hocaoglu M, Sayman Muslubas I, Arf S, Yildiz E, Karacorlu M. Artifact-removed quantitative analysis of choriocapillaris flow voids. *Turk J Ophthalmol*. 2023;53(1):37–43. doi:10.4274/tjo.galenos.2022.23855.
95. Kamei T, Ooto S, Uji A, Ichioka A, Tsujikawa A. Choriocapillaris structure in the fellow eyes of patients with neovascular age-related macular degeneration: an OCT angiography image averaging study. *Retina*. 2023;43(2):286–293. doi:10.1097/IAE.0000000000003660.
96. Kar D, Corradetti G, Swain TA, et al. Choriocapillaris impairment is associated with delayed rod-mediated dark adaptation in age-related macular degeneration. *Invest Ophthalmol Vis Sci*. 2023;64(12):41. doi:10.1167/iovs.64.12.41.
97. Kim JT, Jun JH, Lee SC, Lee MW. Retinal microvasculature and choriocapillaris impairments according to the stage of dry age-related macular degeneration. *Clin Exp Ophthalmol*. 2023;51(1):36–43. doi:10.1111/ceo.14165.
98. Li J, Liu Z, Lu J, et al. Decreased macular choriocapillaris perfusion in eyes with macular reticular pseudodrusen imaged

with swept-source OCT angiography. *Invest Ophthalmol Vis Sci*. 2023;64(4):15. doi:10.1167/iovs.64.4.15.
99. Nagai N, Mushiga Y, Ozawa Y. Retinal pigment epithelial abnormality and choroidal large vascular flow imbalance are associated with choriocapillaris flow deficits in age-related macular degeneration in fellow eyes. *J Clin Med*. 2023;12(4):1360. doi:10.3390/jcm12041360.
100. Narnaware SH, Bansal A, Bawankule PK, Raje D, Chakraborty M. Vessel density changes in choroid, choriocapillaries, deep and superficial retinal plexues on OCTA in normal ageing and various stages of age-related macular degeneration. *Int Ophthalmol*. 2023;43(10):3523–3532. doi:10.1007/s10792-023-02758-3.
101. Abdolrahimzadeh S, Zweifel SA, Di Pippo M, Bajka A, Scuderi G, Lotery AJ. Central macular choriocapillaris impairment as a manifestation of microvascular disease in eyes with subretinal drusenoid deposits. *Eye (Lond)*. 2024;38(1):173–178. doi:10.1038/s41433-023-02654-1.
102. Alagorie AR, Corradetti G, Byon I, et al. Impact of slab selection on the relationship between choriocapillaris flow deficits and enlargement rate of geographic atrophy. *Eye (Lond)*. 2024;38(5):847–852. doi:10.1038/s41433-023-02788-2.
103. Brinkmann M, Viggiano P, Boscia G, et al. Analysis of choriocapillaris reperfusion topography following faricimab treatment for neovascular age-related macular degeneration in therapy-naive patients. *Ophthalmol Ther*. 2024;13(7):1981–1992. doi:10.1007/s40123-024-00967-2.
104. Crincoli E, Catania F, Labbate G, et al. Microvascular changes in treatment-naive nonexudative macular neovascularization complicated by exudation. *Retina*. 2024;44(10):1679–1687. doi:10.1097/IAE.0000000000004194.
105. Greig EC, Moult EM, Despotovic IN, et al. Assessment of choriocapillaris flow prior to nascent geographic atrophy development using optical coherence tomography angiography. *Invest Ophthalmol Vis Sci*. 2024;65(1):33. doi:10.1167/iovs.65.1.33.
106. Kar D, Amjad M, Corradetti G, et al. Choriocapillaris impairment, visual function, and distance to fovea in aging and age-related macular degeneration: ALSTAR2 baseline. *Invest Ophthalmol Vis Sci*. 2024;65(8):40. doi:10.1167/iovs.65.8.40.
107. Nam J, Nivison-Smith L, Trinh M. Spatial analysis reveals vascular changes in retinal and choroidal vessel perfusion in intermediate AMD with reticular pseudodrusen. *Invest Ophthalmol Vis Sci*. 2024;65(2):33. doi:10.1167/iovs.65.2.33.
108. Romano F, Ding X, Yuan M, et al. Progressive choriocapillaris changes on optical coherence tomography angiography correlate with stage progression in AMD. *Invest Ophthalmol Vis Sci*. 2024;65(8):21. doi:10.1167/iovs.65.8.21.
109. Romano F, Vingopoulos F, Yuan M, et al. Decreased macular choriocapillaris perfusion correlates with contrast sensitivity function in dry age-related macular degeneration. *Ophthalmol Retina*. 2024;8(12):1140–1150. doi:10.1016/j.oret.2024.06.005.
110. Sacconi R, Fazzari G, Capuano V, et al. Pachy-reticular pseudodrusen. *Ophthalmol Retina*. 2024;8(11):1066–1073. doi:10.1016/j.oret.2024.05.020.
111. Toma C, Gatti V, Servillo A, et al. Early choriocapillaris dysfunction in fellow eyes of patients with unilateral neovascular age-related macular degeneration. *Eur J Ophthalmol*. 2025;35(3):1054–1060. doi:10.1177/11206721241293494.
112. Zhang Q, Shi Y, Zhou H, et al. Accurate estimation of choriocapillaris flow deficits beyond normal intercapillary spacing with swept source OCT angiography. *Quant Imaging Med Surg*. 2018;8(7):658–666. doi:10.21037/qims.2018.08.10.
113. Scharf J, Corradetti G, Corvi F, Sadda S, Sarraf D. Optical coherence tomography angiography of the choriocapillaris in age-related macular degeneration. *J Clin Med*. 2021;10(4):751. doi:10.3390/jcm10040751.
114. Ledesma-Gil G, Fernandez-Avellaneda P, Spaide RF. Swept-source optical coherence tomography angiography image compensation of the choriocapillaris induces artifacts. *Retina*. 2020;40(10):1865–1872. doi:10.1097/IAE.0000000000002866.
115. Uji A, Balasubramanian S, Lei J, Baghdasaryan E, Al-Sheikh M, Sadda SR. Choriocapillaris imaging using multiple en face optical coherence tomography angiography image averaging. *JAMA Ophthalmol*. 2017;135(11):1197–1204. doi:10.1001/jamaophthalmol.2017.3904.
116. Hiya FE, Cheng Y, Shen M, et al. A novel grid strategy for correlating focal macular anatomic changes with focal changes in choriocapillaris perfusion. *Invest Ophthalmol Vis Sci*. 2024;65(14):5. doi:10.1167/iovs.65.14.5.
117. Chu Z, Cheng Y, Zhang Q, et al. Quantification of choriocapillaris with phansalkar local thresholding: pitfalls to avoid. *Am J Ophthalmol*. 2020;213:161–176. doi:10.1016/j.ajo.2020.02.003.
118. Berni A, Shen M, Cheng Y, et al. The total macular burden of hyperreflective foci and the onset of persistent choroidal hypertransmission defects in intermediate AMD. *Am J Ophthalmol*. 2024;267:61–75. doi:10.1016/j.ajo.2024.06.023.
119. Laiginhas R, Liu J, Shen M, et al. Multimodal imaging, OCT B-scan localization, and en face OCT detection of macular hyperpigmentation in eyes with intermediate age-related macular degeneration. *Ophthalmol Sci*. 2022;2(2):100116. doi:10.1016/j.xops.2022.100116.
120. Liu J, Laiginhas R, Shen M, et al. Multimodal imaging and en face OCT detection of calcified drusen in eyes with age-related macular degeneration. *Ophthalmol Sci*. 2022;2(2):100162. doi:10.1016/j.xops.2022.100162.
121. Berni A, Kastner JD, Shen M, et al. Hyperreflective foci along the retinal pigment epithelium predict the onset of large choroidal hypertransmission defects in age-related macular degeneration. *Am J Ophthalmol*. 2025;274:76–90. doi:10.1016/j.ajo.2025.02.021.
122. Berni A, Cheng Y, Shen M, et al. Updated guidelines for imaging the choriocapillaris in eyes with age-related macular degeneration using swept-source oct angiography. *Am J Ophthalmol*. 2025 Jun 1 [online ahead of print].